Research Article

A facile hydrolysis-controllable strategy for fast synthesis of Ti-MWW with steam-environment crystallization method

Feilan Huang[1] · Mengru Li[2] · Shujuan Guo[3] · Xiaohui Chen[1]

Received: 26 May 2020 / Accepted: 7 October 2020 / Published online: 5 December 2020

Abstract
Numerous strategies have been developing to synthesis the Ti-MWW zeolites, but more effective synthesis process is still a significant challenge. In our study, with the synergy of PI and IPA (Isopropyl Alcohol) , the Ti-MWW zeolites with adjustable active sites were directly developed by titanium-silicon composite with homodisperse titanium species in the continuous circulation of SDA steam. The Ti-MWW achieved were flaky nanocrystal Ti-MWW with the size of 20–400 nm, and the mesopores with ca. 20 nm pore size and 0.76 $cm^3\ g^{-1}$ total pore volumes were simultaneously created, and the crystallization period was decreased to 2 days for a comparison with 7–14 days required in conventional method. Furthermore, the catalytic tests showed that Ti-MWW exhibit a higher activity almost 7 times than Ti-MWW prepared by conventional dry–gel method in the liquid-phase epoxidation of 1-hexene with hydrogen peroxide due to the improved accessibility of the active sites inside the crystals and the number of active sites. The physicochemical properties were analyzed by XRD, SEM, BET, UV–Vis, FT-IR, ICP et al., and the mechanism for incorporation of titanium species into framework have been investigated in details. This facile and efficient synthetic strategy would considerably facilitate the preparation of zeolites with high catalytic performance in industrial production on a large-scale in the future.

Keywords Ti-MWW · Hydrolysis-controllable · One-step · Steam-assisted conversion · 1-hexene epoxidation

1 Introduction

Zeolites are crystalline micropores materials with unique molecular size pore topology and high surface areas, have received extensive attention and been applied in traditional area of adsorption, catalysis fields and potential application in biomass-transformation [1–3]. Titanium silicates with isolated and tetrahedrally coordinated Ti^{4+} ions in zeolite frameworks are efficient catalysts for selective oxidation of a large family of organic substrates [4]. Owing to the unique structure composed of large 12-MR supercages ($0.7 \times 0.7 \times 1.8$ nm) and independent 10-MR channels, a novel titanosilicate Ti-MWW developed successfully by Wu [5–9] exhibits superior catalytic performance in the epoxidation of linear alkenes in contrast to classical TS-1 [10]. In addition, MWW zeolites are quite versatile which were used to obtain modified MWW-type materials (expansion, delamination, pillarization, desilication) [11–14].

To further improve the activity, such as Ti-YNU-1 [15] and Ti-MCM-36 [16, 17] has been synthesized from MWW-type precursor through interlayer expanding, and pillaring, respectively. Moreover, Re-Ti-MWW-PI [18, 19] was hydrothermally synthesized via post-synthesis treated the Ti-MWW with organic amines exhibit much higher activity than conventional Ti-MWW-HTS in the epoxidation of alkenes. Nevertheless, in spite of the excellent catalytic performance in oxidation of bulky molecules, there is

✉ Xiaohui Chen, chenxhfzu@fzu.edu.cn | [1]National Engineering Research Center of Chemical Fertilizer Catalyst, School of Chemical Engineering, Fuzhou University, Fuzhou 350002, Fujian, People's Republic of China. [2]School of Chemical Engineering, Fuzhou University, Fuzhou 350116, Fujian, People's Republic of China. [3]Ocean College, Minjiang University, Fuzhou 350108, Fujian, People's Republic of China.

SN Applied Sciences (2020) 2:2157 | https://doi.org/10.1007/s42452-020-03643-9

still a significant challenge for the directly synthesis of Ti-MWW zeolite due to its complex 3D framework structure [20]. Furthermore, the preparation of Ti-MWW is typically under hydrothermal conditions, where a large amount of solvents is necessary, which accompanied with a lot of shortcomings such as high energy consumption and long crystallization period caused by the low utilization efficiency of the nutrients of silicates [8, 21–23]. To overcome this issue, green synthesis methods such as dry–gel and solvent-free method have been successfully developed [23–27]. Zhang's group [25] and Xiao's group [23, 26, 27] had done a lot of work in green synthesis of zeolites with different structures such as MFI, BEA, EUO, CHA, SAPO and TON by solvent-free method, which offer a more effective way to the synthesis of zeolites. However, these methods are proposed in the presence of fluoride medium, which is unfriendly to environment. Wu [24] et al. prepared Ti-MWW zeolites by one-step dry–gel method exhibited a poor catalytic performance due to its large crystal sizes and the lower incorporation of titanium species, which greatly restrict large-scale industrial application. Hence, zeolites with small crystals are more needed in catalytic reactions. Furthermore, due to the titanium species can't be directly incorporated into MWW framework [28] and the precipitation of the oxides of titanium outside the lattice framework during the synthesis of titanosilicate zeolites [29], the direct dry gel synthesis of Ti-MWW is still a challenge. Therefore, it is of great significance to develop a facile, green and effective strategy to synthesize nanosized Ti-MWW zeolite.

Thangaraj [29, 30] et al. had reported that lower incorporation of Ti is due to the precipitation of TiO_2 during the preparation of the precursor mixture or during the crystallization of the precursor gel, namely, zeolites exhibit low catalysis performance even though with the highly crystalline. TS-1 with more Ti content was successfully synthesized using IPA as an organic solvent to avoid the precipitation of TiO_2 by matching the rate of hydrolysis between the Ti-alkoxides in the process of hydrothermal synthesis. Based on these points, a uniformly dispersed titanium-silicon composite has been synthesized by controlling the dispersion of titanium species effectively, which can be used as the nutrients for the preparation of nanosized Ti-MWW. The nanosized Ti-MWW performed with more framework Ti species due to the low mobility of Ti species during the steam-environment conversion procedure, which prevent the agglomeration of titanium species in the titanium-silicon precursor, the aggregated amorphous particles were directly crystallized in situ to convert into flaky zeolite nanocrystals, and a structure was generated at the same time. Further, the synthesis time was also reduced considerably due to crystallization occurred at the solid–liquid interface with high SDA concentration. A possible synthesis mechanism of the nanosized Ti-MWW prepared with titanosilicate was proposed on the basis of structural characterizations. Furthermore, the nanosized Ti-MWW exhibited better catalytic performance in the epoxidation of 1-hexene while compared with the conventional dry–gel method due to the more catalytic active sites and better accessibility.

2 Experimental

2.1 One-step synthesis of Ti-MWW

The one-step synthesis of Ti-MWW was produced by the following steps: first, SiO_2 (A200, Degussa), the seeds (with 10 wt% SiO_2) and boric acid (H_3BO_3, AR (Analytical Reagents)) were mixed together, further dissolved in an aqueous solution of piperidine (PI, AR) to obtain a homogenous gel named solution A. Then, tetrabutyl titanate (TBOT, AR) was dispersed in isopropanol (IPA, AR) under vigorous stirring to obtain mixed solution B. Next, the solution B was dropped into solution A carefully under continued stirring, and further stirred for 2 h to form the resultant homogeneous gel with the composition of 1 SiO_2: 0.02 TiO_2: 0.1 B_2O_3: (0, 0.27, 0.53, 1.23) PI: (0, 0.975, 1.95, 4) IPA. The resultant gel was completely evaporated to get the dry gel over an oil bath under magnetic stirring at 353 K. The powder was transferred into a small container which was placed in a special Teflon-lined autoclave where piperidine and water were situated on the bottom. The small container was put into Teflon-lined autoclave, and crystallized statically at 443 K for 0–5 d. The product was washed with deionized water and drying at 383 K denoted as Ti-MWW-P. Subsequently, Ti-MWW-P were treated with 2.0 mol·L^{-1} HNO_3 aqueous solution for 12 h to extract the extra-framework Ti together with a portion of framework B. The after acid-treatment samples were further dried at 383 K and calcined at 823 K for 6 h to obtain the white solids denoted as Ti-MWW.

2.2 Catalyst characterization

The change in the MWW phase structure was characterized by X-ray diffraction spectroscopy (XRD, PANalytical Axios Petro diffractometer) using Cu-Kα radiation under the setting conditions of 45 kV and 40 mA. The typical physico-chemical properties of the zeolites were analyzed by BET method using Micrometric ASAP 2020 M. Micromorphology of the samples was characterized by Hitachi S-4800 scanning electron microscope (SEM). The UV–Vis diffuse reflectance spectra were recorded on a Lambda 950 spectrophotometer using $BaSO_4$ as the reference. The FT-IR analysis of catalysts were carried out by Thermo

Fisher Scientific Nicolet 6700. The content of Ti was determined by PerkinElmer inductively coupled plasma-optical emission spectroscopy OPTIMA 8000 (ICP). The thermogravimetric of as-prepared samples were performed with a Setsys Evolution TGA synchronous thermal analyzer at a heating rate of 10 °C/min in an atmosphere containing 80% N_2 and 20% O_2.

2.3 Catalytic activities

The catalytic performance was evaluated by the epoxidation reaction of 1-hexene with hydrogen peroxide in a 25 mL glass flask with a water condenser under appropriate stirring. 10 mmol 1-hexene (99%, AR), 10 mmol H_2O (30% aqueous solution, AR), 50 mg catalysts and 10 mL of acetonitrile (99%, AR) were mixed and stirred in the flask at 333 K for 2 h. The solid samples were removed from the reaction system by centrifugation, and the final reaction mixture was analyzed by a gas chromatograph (Agilent 6890) while the remaining of unconverted H_2O_2 was quantified by iodometry method with 0.1 mol·L^{-1} Sodium Thiosulfate.

3 Results and discussion

3.1 Characterization of Ti-MWW zeolite

In this work the influence of dry gel composition, the crystallization condition and the crystallization period were investigated during the synthesis procedure of Ti-MWW zeolites and listed in (Table 1) respectively. As shown in Table 1 the crystallization period and piperidine concentration in the DGC environment play an important part in synthesis of Ti-MWW. Different from the DGC method reported by Wu, IPA and PI (No.8 and No.9) showed great prospect in preventing Ti atoms from hindering MWW crystallization process.

3.1.1 Synthesis of Ti-MWW zeolite with different aging temperature

Since the effect of temperature on hydrolysis is crucial, we have studied the effect of aging temperature on the preparation process (Fig. 1). The dry gels all exhibited a

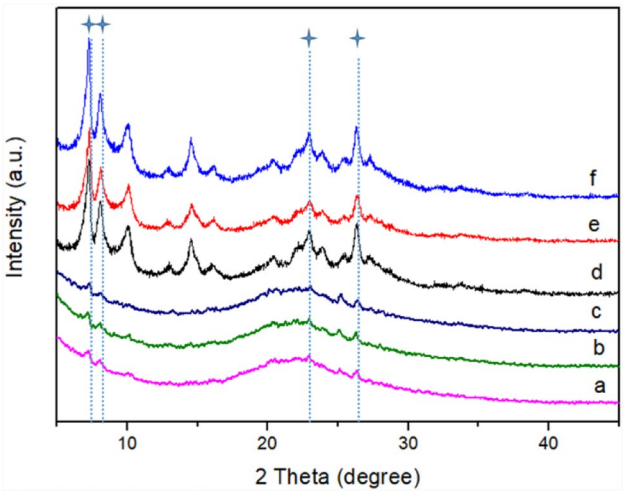

Fig. 1 The XRD patterns of the dry gels and Ti-MWW zeolites with different aging temperatures (Table 1, No. 2, No. 4, No. 5). Dry gels: (a) 0 °C, (b) room temperature, (c) 45 °C, Ti-MWW: (d) 0 °C, (e) room temperature, (f) 45 °C

Table 1 Different recipes for the synthesis of Ti-MWW zeolites

Entry	gel composition[a]		Aging temperature	Crystallization condition[b]			Product type
	Si/PI	Si/IPA		Si/H_2O	Si/PI	Period (d)	
No.1	1.89	0.51	RT[c]	0.4	1.4	1	Amor[d] + MWW
No.2	1.89	0.51	RT	0.4	1.4	2	MWW
No.3	1.89	0.51	RT	0.4	1.4	5	MWW
No.4	1.89	0.51	0 °C	0.4	1.4	2	MWW
No.5	1.89	0.51	45 °C	0.4	1.4	2	MWW
No.6	0.81	0.51	RT	0.4	∞	2	Amor
No.7	3.70	0.51	RT	0.4	1.4	2	MWW
No.8	∞	0.51	RT	0.4	1.4	2	MWW
No.9	1.89	∞	RT	0.4	1.4	2	MWW
No.10	1.89	1.05	RT	0.4	1.4	2	MWW
No.11	1.89	0.25	RT	0.4	1.4	2	MWW

[a]other composition of homogeneous gel: 1 SiO_2: 0.1 B_2O_3: 0.05 TiO_2

[b]further crystallized at 443 K for 2 days

[c]RT: room temperature

[d]Amor: amorphous

broad diffraction peak at 2θ of around 22.0° are attributed to amorphous silica, while the small diffraction peaks at 2θ of about 7.2°, 7.92°, 22.44° and 26.42° can be ascribed to the seeds (Fig. 1). The Ti-MWW exhibited well-resolved diffraction peaks characterized by the MWW topology and the crystallinity of zeolites basically unchanged with the increase of aging temperature (Fig. 1).

As an effective method to detect the surface morphology of molecular sieve, SEM was used to further observe the crystallization of Ti-MWW zeolites. Figure 2 shows that the Ti-MWW zeolites prepared with different aging temperatures were typical flaky structures with the size was comparable to that obtained by hydrothermal method, and the sizes of Ti-MWW zeolites was slightly lager with the increase of aging temperature, which can be attributed to the dissolution of silica during aging procedure, the results were in agreement with those obtained from the XRD patterns (Fig. 1).

The textural properties of zeolite are generally regarded as one of the most important characteristics. Herein, to understand the physical structure of Ti-MWW prepared by this one-step SEC method comprehensively, nitrogen adsorption–desorption tests were carried out on the samples and the results are shown in Fig. 3 and Table 2.

As show in Fig. 3A, the sorption isotherms of all the samples were Type I isotherms (Fig. 3), which were the characteristic of microporosity. The increases in the adsorption volumes at high partial pressure were also observed on the Ti-MWW zeolites, these mesopores were likely attributed to the non-rigid aggregates of plate-like particles or crystal defects. So, the Ti-MWW showed similar physicochemical properties, this is consistent with the pore volume showed in Table 2. Meanwhile, the hysteresis loops at relative pressure 0.4–1.0 are tend to typical H_4 hysteresis loops, suggesting the presence of obvious mesoporous in the samples. As shown in Fig. 3B, the pore diameter distribution calculated by the Barrett–Joyner–Halenda (BJH) method reveals that the samples have a broad pore size distribution in the range of 2–140 nm, indicating that the samples possess abundant mesopores and macropores, and all the samples exhibited considerable pore distribution peak centered at about 20 nm, which can be ascribed to the intergranular mesopores resulted from the migration and aggregation of primary nanosized flaky crystals [31], the result is corresponding to the porous parameters summarized in Table 2.

Table 2 exhibits the textural properties of Ti-MWW zeolites prepared by one-step SEC method and traditional

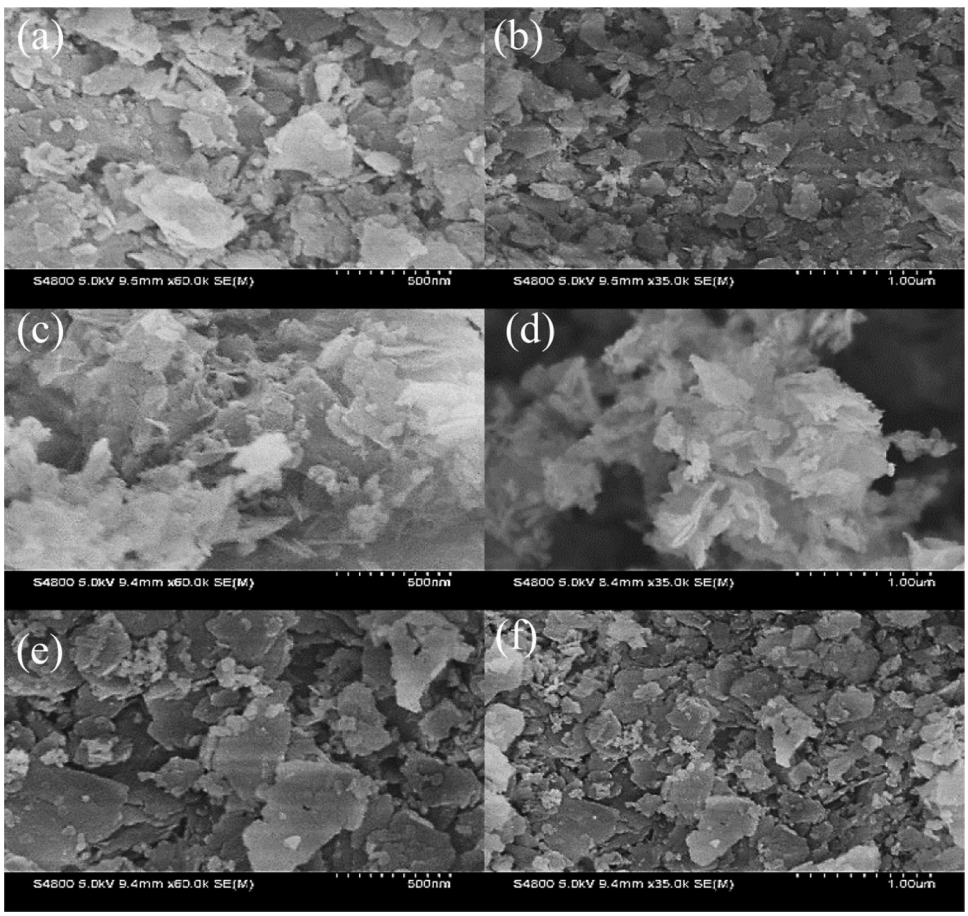

Fig. 2 The SEM imagines of Ti-MWW zeolites with different aging temperature (Table 1, No. 2, No. 4, No. 5). **a, b** Ti-MWW at 0 °C, **c, d** Ti-MWW at room temperature, **e, f** Ti-MWW at 45 °C

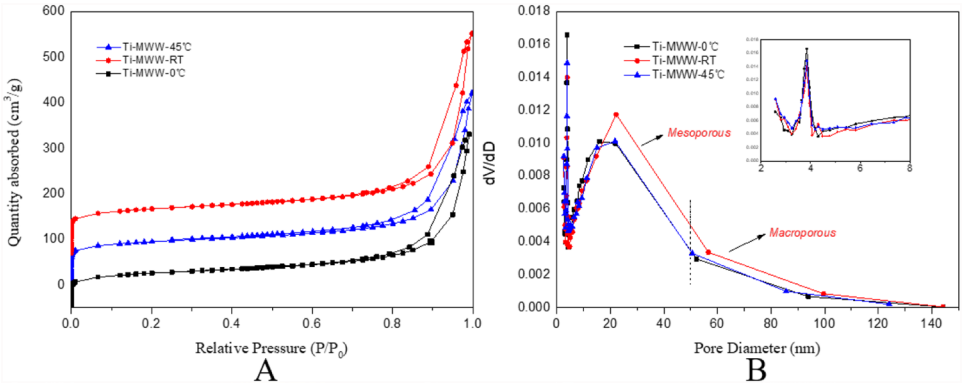

Fig. 3 N_2 adsorption–desorption isotherms (a) and pore size distributions, (b) of Ti-MWW zeolites with different aging temperature

Table 2 Textural properties of Ti-MWW zeolite prepared with different aging temperature[a]

Samples	Surface area (m^2 g^{-1})	Pore volume (cm^3 g^{-1})[b]			Average pore diameter (nm)
		Total	Micro	Meso	
Ti-MWW-0 °C	296.57	0.65	0.08	0.57	19.08
Ti-MWW-RT	319.98	0.76	0.10	0.66	20.32
Ti-MWW-45 °C	283.37	0.61	0.09	0.52	18.47
Ti-MWW[c]	352	0.44	0.16	0.28	9.78

[a]other synthesis conditions were the same except for aging temperature

[b]the volume of micropores from the t-plot ($cm^3 \cdot g^{-1}$)

[c]prepared by traditional method [32]

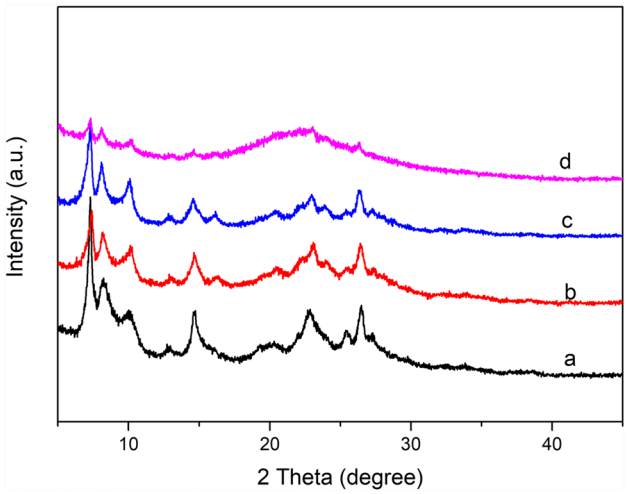

Fig. 4 The XRD patterns of Ti-MWW synthesized with different Si/PI (Table 1, No. 2, No. 6–8). (a) Si/PI = ∞ (No. 8), (b) Si/PI = 3.7 (No. 7), (c) Si/PI = 1.89 (No. 2), (d) without PI on bottom (No. 6)

method, separately. It can be found that the Ti-MWW samples prepared by one-step SEC method exhibit excellent pore structure, in which the mesopore volume and average pore diameter of Ti-MWW prepared by aging at room temperature is 0.66 cm^3 g^{-1} and 20.32 nm, which is twice than the values of boron-containing Ti-MWW prepared by conventional methods. Through the analysis above, it can be seen that the Ti-MWW zeolites prepared by one-step SEC method exhibit a superior pore structure, namely, hierarchical structure. That is to say, the hierarchical nanosized Ti-MWW zeolite with Meso- and microporosity has been obtained without post-treatment, and such the abundant mesopores of the Ti-MWW zeolite is of great importance for catalytic application, which are beneficial to the mass transport and the accessibility of active sites.

3.1.2 Effects of PI in both synthetic gel and bottom of the Teflon-lined

In this work, the function of PI was divided into two parts, one was act as protect agent of TBOT forming colloid Ti species and prevent it from further hydrolysis during the evaporation step. In the other hand, it was served as template agent assembling amorphous SiO_2 to MWW type zeolite. Herein, the effect of PI at different parts on the synthesis of Ti-MWW zeolites were investigated.

Figure 4d shows that the Ti-MWW prepared without PI on the bottom of the Teflon-lined exhibit a basically amorphous substance (Table 1, No.6), this proves that the PI added on the bottom of Teflon-lined is essential for synthesis procedure to serve as structure directing agent. Figure 4a-c shows the crystallinity of the Ti-MWW zeolites prepared with different amount of PI in synthetic gel (Table 1, No. 2, 7, 8), the samples exhibit a series of characteristic diffraction peaks attributing to typical MWW zeolite framework and no other phase appeared indicating that Ti-MWW has been prepared successfully and different PI content in the synthetic gel has negligible effect on the crystal structure of Ti-MWW doped, but it has a significant effect on the crystallinity caused. But the UV–Vis and FT-IR spectroscopy showed in Fig. 5A and B indicate that PI in dry gel precursor have great

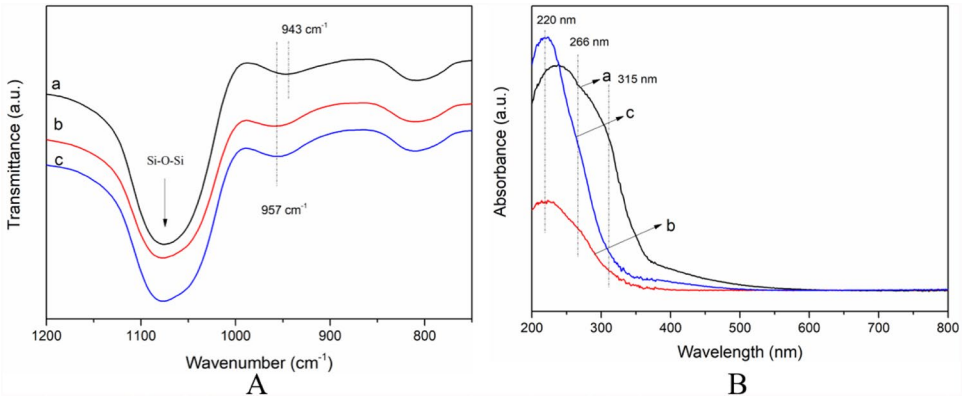

Fig. 5 FT-IR (**A**) and UV–Vis diffuse reflectance, (**B**) spectra of the Ti-MWW zeolite with synthesized with different Si/PI. **a** Si/PI = ∞ (No. 8), **b** Si/PI = 3.7 (No. 7), **c** Si/PI = 1.89 (No. 2)

influence on the state of titanium during the synthesis procedure.

The tetrahedrally coordinated Ti species were considered to serve as the active components on the selective oxidation reactions commonly. Thus, the FT-IR spectra (Fig. 5 A) and UV–Vis spectra (Fig. 5B) are collected to investigate the titanium coordination in the Ti-MWW samples prepared with different Si/PI.

The IR spectra of Ti-MWW (Table 1, sample No. 8) without the addition of PI in synthetic gel depicted in Fig. 5A a shows a characteristic band at 943 cm^{-1} which is related with the residual framework B [7], and the Fig. 5A b-c show a characteristic band at 957 cm^{-1} which can be attributed to the stretching vibration of four-coordinated Ti species in the zeolite framework, and the intensity of peak at 957 cm^{-1} become stronger with the increase of PI in synthetic gel precursor [33]. This can be attributed to the fact that the addition of PI in synthetic gel can protect the hydrolysis of TBOT to avoid the precipitation of TiO_2. Namely, the PI in synthetic gel is a crucial factor for incorporation of Ti atoms into the framework of MWW-type zeolite.

Figure 5B shows the difference of characteristic absorption bands in UV–Vis spectra which are related to different coordination state of titanium in different environments. The UV–Vis spectra of Ti-MWW (Table 1, sample No. 8) depicted in Fig. 5B a shows a broad peak at ca. 266 nm with a shoulder peak at ca. 320 nm, which indicated that a large amount of Ti species existed in the form of pentacoordinate Ti species, oligomeric octahedral Ti species and anatase phases [34]. On the other hand, Fig. 5B b-c show a main peak at ca. 220 nm and a weak peak at ca. 266 nm, while the band at 226 nm had been widely acknowledged as the evidence of tetrahedral coordinated Ti in zeolite framework [28], and the peak at ca. 266 nm become weaker with the decrease of PI amount in synthetic gel precursor. Therefore, considering the framework Ti species, Si/PI = 1.89 in synthetic gel is selected as the best ration. The literature shows: The 220 nm peak in the UV–Vis spectrum of Ti-MWW molecular sieve is attributed to the isolated framework four-coordinated titanium active center. Non-framework titanium usually exhibits an absorption peak at around 260 nm. The absorption peak of titanium ore is around 320 nm. The UV–Vis spectra of samples prepared under different Si/PI conditions are shown in Fig. 6. When no PI is added to the mixed gel, the synthesized Ti-MWW molecular sieve shows a broad peak at 220–330 nm, which indicates that the molecular sieve It may contain five coordinated titanium species, oligomeric octahedral titanium species, and anatase and other different types of titanium species; with the increase of PI content in the mixed gel, the absorption peak gradually narrows, showing a 220 nm The main peak and the shoulder peak at 266 nm; when the PI content in the mixed gel continues to increase, the absorption peak at 220 nm gradually concentrates and becomes sharper. This result shows that as the PI content in the gel solution increases, the Ti species entering the MWW framework will also increase. This may be because the increase in PI content

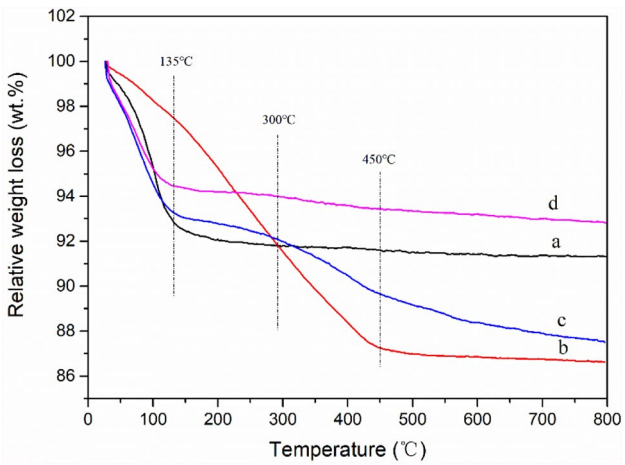

Fig. 6 TG curves of the different samples. (a) Dry gel of (No.8), (b) dry gel of (No.2), (c) as-synthesized Ti-MWW (No.2), (d) Ti-MWW (No.2)

protects TBOT from direct contact with the water phase and instantaneously hydrolyzes to form TiO_2 precipitation, avoiding the waste of titanium source, so that more effective titanium species.

In to the molecular sieve framework to form four-coordinated titanium. Therefore, from the perspective of effective Ti species, Si/PI = 1.89 in the mixed gel is selected as the better choice for making Ti-MWW molecular sieve.

Figure 6 shows the TG curves of different samples. It is evident that all the samples exhibited weight loss below 135 °C, attributing to the removal of water adsorbed on the surface of particles and occluded in inter-mesoporous and macropores. Figure 6a shows the TG curve of dry gels of Ti-MWW without PI (Table 1, No.8), Fig. 6b shows the TG curve of dry gels Ti-MWW with homogeneous gel composition of Si/PI = 1.89 (Table 1, No.2), Fig. 6c shows the TG curve of as-synthesized Ti-MWW (without acid treatment and calcination) (Table 1, No.2), Fig. 6c shows the TG curve of Ti-MWW(Table 1, No.2). Figure 6b exhibits two stages of weight losses at about 25–135 °C and 135–450 °C, which are corresponded to the removal of physically adsorbed water and the decomposition of PI, respectively, while the Fig. 6a show the weight loss only below 135 °C. Figure 6c exhibits two weight losses of about 1% and 4% at around 135–300 °C and 300–800 °C which are belong to the decomposition of PI molecules located in layers and intralayer sinusoidal 10-ring channels, respectively [19]. Namely, the PI can be occluded in silicate during the preparation of the dry gels, but the PI remained in dry gel is no sufficient to support the crystallization at 170 °C which is corresponding to the result showed in Fig. 4d. This conclusion is essential for subsequent synthesis of Ti-MWW.

3.1.3 Effects of IPA of the synthetic gel

In our work, many kinds of organic alcohols were selected to protect TBOT from its immediate hydrolysis, of which IPA performed best. The samples prepared with different Si/IPA exhibit a series of characteristic reflections assigning to typical MWW zeolite framework (Fig. 7), and the slightly increase of diffraction peaks illustrated that IPA had negligible impact on the crystallinity of Ti-MWW.

The FT-IR spectra of Ti-MWW prepared with different Si/IPA was depicted in Fig. 8A shows the intensity of characteristic band at ca. 960 cm^{-1}, as the evidence of framework Ti species. Figure 8B show the UV–Vis diffuse reflectance spectra of Ti-MWW synthesized with different Si/IPA, it is worth noting that all the samples exhibit a main band at ca. 220 nm, while the Ti-MWW with IPA/Si = 4 (sample No.11) shows another obvious band at 325 nm, which indicated that a large amount of Ti species in sample No.11 existed in the form of penta-coordinate Ti species, oligomeric octahedral Ti species and anatase phases. The

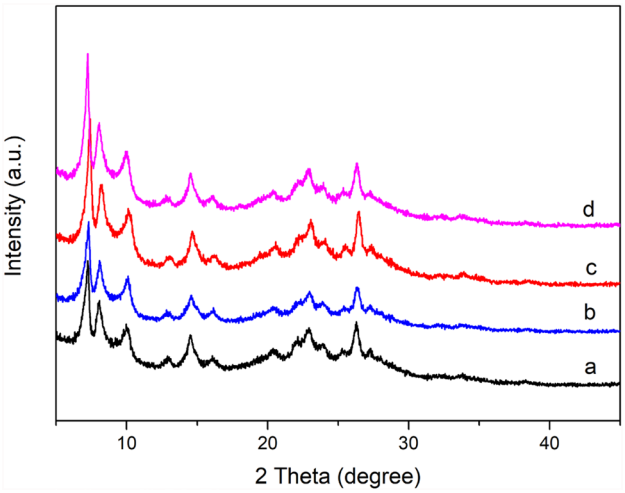

Fig. 7 The XRD patterns of Ti-MWW synthesized with different Si/IPA (Table 1, No. 2, No. 9–11), **a** IPA/Si = 0 (No. 9), **b** IPA/Si = 0.95 (No. 10), **c** IPA/Si = 1.96 (No. 2), **d** IPA/Si = 4 (No. 11)

evaporated rate of precursor can be controlled by adjusting the amount of IPA in synthetic gel precursor, which may influent the incorporate of Ti species in framework. The phenomenon can be attributed to the rate of hydrolysis of Ti-alkoxide in synthetic gel, and the hydrolysis rate is matching with the evaporation rate of the synthetic gel. In the synthesis procedure, the TBOT is added in IPA to improve its' dispersion, and during the evaporation procedure, the evaporation rate was raising with the increase of IPA in synthetic gel, and the hydrolysis rate of the Ti-alkoxide is consistent with the rate of evaporation. When the IPA/Si = 4, the hydrolysis rate of the Ti-alkoxide is so fast to produce the TiO_2, leading to poor incorporation of Ti in the lattice. Therefore, the IPA in synthetic gel not only improve the dispersion of Ti species but also control the evaporation rate to avoid the instantaneous hydrolysis of TBOT to the hydroxide.

3.1.4 Effect of crystallization period

To investigate the formation mechanism of Ti-MWW zeolite with intra- and inter-crystalline mesoporous structure, a series of samples with different crystallization period were prepared during steam-environment at 170 °C.

Figure 9 shows the X-ray diffraction patterns of Ti-MWW zeolite prepared with different crystallization period. Without the steam-environment treatment, the XRD pattern of Ti-MWW-0 d exhibits a broad peak around 23° corresponded to the amorphous structure of small silica particles (Fig. 10a). The characteristic diffraction peaks corresponding to typical MWW framework begins to appear after 1 day of steam-environment treatment, and the crystallinity of Ti-MWW zeolite gradually increased with the

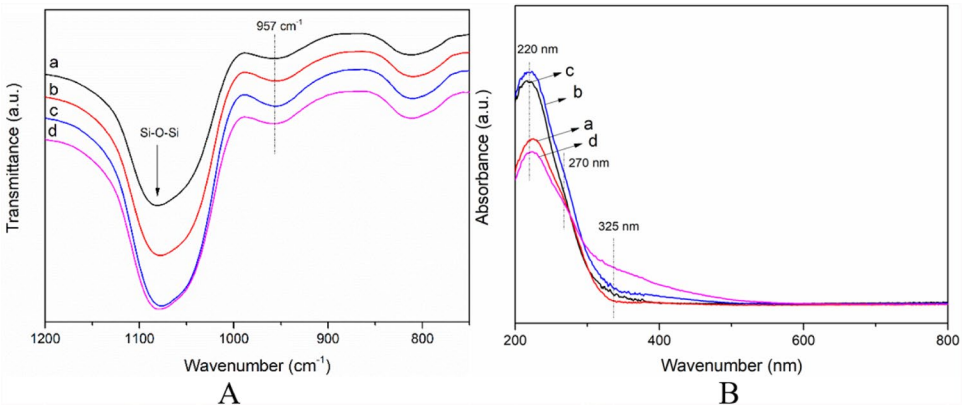

Fig. 8 The FT-IR (**A**) and UV–Vis diffuse reflectance (**B**) spectra of Ti-MWW synthesized with different Si/IPA(Table 1, No. 2, No. 9–11), **a** IPA/Si = 0 (No. 9), **b** IPA/Si = 0.95 (No. 10), **c** IPA/Si = 1.96 (No. 2), **d** IPA/Si = 4 (No. 11)

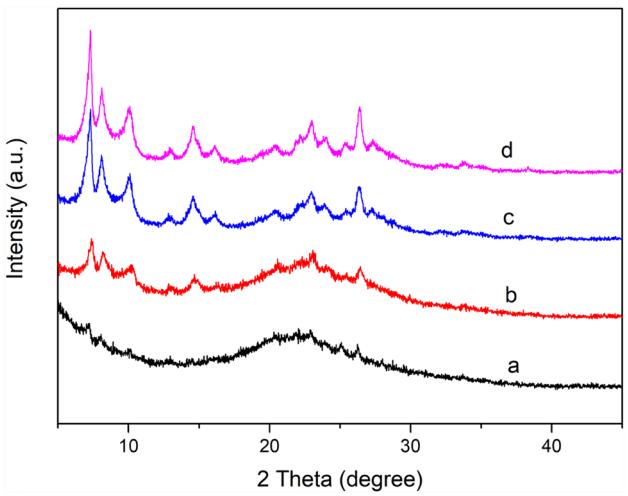

Fig. 9 XRD patterns of Ti-MWW with Si/PI = 1.89, Si/IPA = 0.51 crystallized with different crystallization period

prolong of the crystallization period, which is corresponding to the most of aggregated small silica particles in Ti-MWW-0 d convert into connected flaky structure gradually (Fig. 10). When the crystallization period over 2 days, the XRD patterns of Ti-MWW does not increase significantly indicating that the crystallization of Ti-MWW has been basically formed within 2 days, the results were consistent with SEM imagines (Fig. 10) that Ti-MWW with typical well-define crystallization of 200–400 nm was transformed from amorphous silica particles within 2 days. Namely, 2 days is the most suitable crystallization period for the prepared of nano-crystalline Ti-MWW zeolite.

Generally, tetrahedrally coordinated Ti species were considered to serve as the active sites for the selective oxidation reactions [34]. Herein, UV–Vis spectroscopic and FT-IR characterization were employed to investigate titanium coordination in the Ti-MWW.

As shown in Fig. 11A a, Ti-MWW-0 d exhibit characteristic IR band at 930 cm^{-1}, which can be attributed to the Ti-specific vibrational frequency in tripodal [$Ti(OSi_3)$OH] species [35], indicating that the titanium silicate species has formed during the aging procedure. Figure 11A b-d show that the other samples prepared with different crystallization times exhibit the characteristic vibration band around 958 cm^{-1}, which can be assigned to the stretching of Si–O-Ti bonds in the perfect tetrapodal [$Ti(OSi)_4$] species [36], and regarded as an evidence of the incorporation of tetrahedral Ti species into zeolite framework during crystallization process, which are consistent with the result of UV–Vis diffuse reflectance spectra (Fig. 11B).

It has been reported by previous studies that titanium species with various coordination states perform different characteristic absorption bands in the UV–vis spectrum, for example, absorption bands at 220 nm correspond to charge transfer from O^{2-} to tetrahedrally coordinated Ti^{4+} which is highly dispersed in the zeolite framework, 260 nm correspond to extra-framework oligomeric octahedral Ti–O–Ti, 320 nm correspond to anatase phase [37, 38]. The UV–Vis diffuse reflectance spectra of the Ti-MWW samples with different crystallization time are shown in Fig. 11B, where illustrate that the titanium species have been incorporated into Ti-MWW gradually with the prolong of the crystallization period. The UV–Vis spectra of Ti-MWW-0d depicted in Fig. 11B a shows a broad peak from 220 to 320 nm, which is attributed to the titanium species with various coordinated state [39]. Furthermore, the characteristic peak become narrow with the increasing of the crystallization time, indicating the shift of coordination state about titanium species. Figure 11B b shows a main band around 220 nm with a weak shoulder around 270 nm, suggesting that titanium species are mainly tetrahedrally coordinated in the framework with a small part of extra-framework TiO_6 species, both Fig. 11B c-d only show a dominant band at 225 nm, demonstrating there are mainly tetrahedrally coordinated framework titanium species in the Ti-MWW-2d and Ti-MWW-5 d. Therefore, 2 days is the suitable period for extra-framework titanium species transformed into MWW framework.

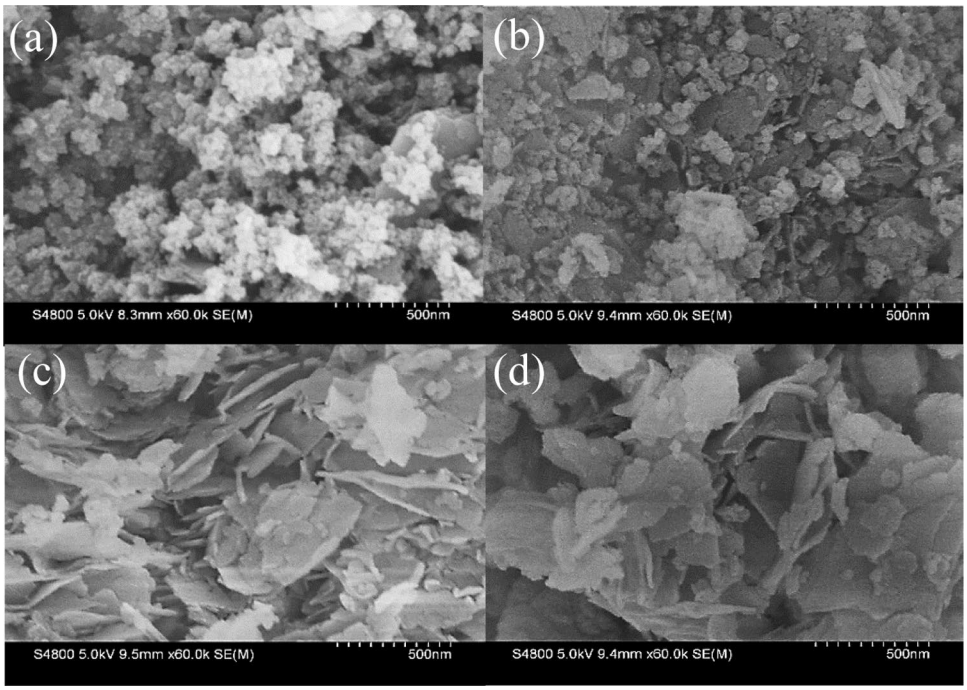

Fig. 10 SEM images of Ti-MWW with Si/PI = 1.89, Si/IPA = 0.51 crystallized with different crystallization period **a** Ti-MWW-0 d, **b** Ti-MWW-1 d, **c** Ti-MWW-2 d, **d** Ti-MWW-5 d

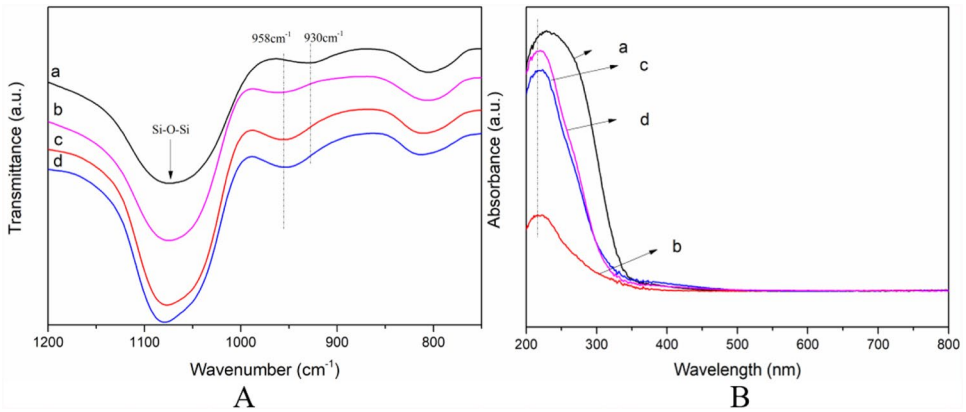

Fig. 11 FT-IR (A) and UV–Vis diffuse reflectance, (B) spectra of the Ti-MWW zeolite with different crystallization period (a) Ti-MWW—0 d, (b) Ti-MWW—1 d, (c) Ti-MWW—2 d, (d) Ti-MWW—5 d

3.2 Catalytic performance and formation mechanism of Ti-MWW zeolite

The catalytic performance of Ti-MWW zeolites synthesized with various conditions was investigated by chosen the epoxidation of 1-hexene with H_2O_2 as the probe reaction (Table 3). The products were mainly the epoxide (> 99%) together with a little amount of its ring-opening product of diol (< 1%) [38]. The results in Table 3 illustrate that the conversion of 1-hexene over Ti-MWW zeolites could reach 28.8%, which was nearly 7 times higher than that of conventional dry–gel Ti-MWW (Table. 3 No.12) [24]. The result can be ascribed to the smaller particle, larger pore volume and higher Ti content of Ti-MWW synthesized by one-step SEC method. The Ti content and catalytic properties of the Ti-MWW are improved with the increase of crystallization period while compared the samples in Table 3 (No. 1 to No.3), this can be attributed to the rigid environment of the active species in framework structure. As for samples with different aging temperature of synthetic gel showed in Table 3 (No. 2, No.4, No.5), their different performance may be attributed to the different Ti content and the accessibility of Ti species. In comparison with the samples of different Si/PI and Si/IPA (Table. 3, No.2, No.6–11), it can be found that PI and IPA are essential in the procedure of synthesizing Ti-MWW, and the sample with the Si/PI = 1.89 and Si/IPA = 1.96 exhibit the highest activity, which show the highest framework Ti species.

During the traditional dry gel method [24], the mix of H_2O_2 and TBOT were used as titanium source in the preparation of dry gels, and the inevitable hydrolysis of titanium occurred during evaporation process, so that Ti was unable

Table 3 Chemical composition of Ti-MWW and the results of epoxidation of 1-hexene with H_2O_2[a]

Samples	Catalysts[b]	Epoxidation of 1-hexene[c]			
	Si/Ti	1-Hexene Conversion (%)	TON[d] (mol(mol)$^{-1}$)	H_2O_2(mol%)	
				Conversion	Efficiency[e]
No. 1	161	3.27	91	5.38	60.8
No. 2	78	28.8	327	34.3	84.0
No. 3	74	27.5	259	34.9	78.8
No. 6	197	1.2	19	2.9	41.4
No. 7	84	15.5	131	29.7	52.5
No. 8	–	0	–	–	–
No. 9	89	14.16	139	23.9	65.1
No. 10	91	16.07	156	24.1	66.7
No. 11	88	19.85	192	27.4	72.4
No. 12[f]	191	4.2	96	8	52.5

[a]Reaction conditions: 1-hexene, 10 mmol; H_2O_2(30 wt.%), 10 mmol; MeCN, 10 mL; catalyst, 50 mg; temperature, 333 K; time, 2 h

[b]Ti-MWW-n: n correspond to the number of the samples in Table 1. The catalysts were calcined

[c]The oxidation product selectivity was over 99% for all the reactions. So the data were thus omitted for clarity

[d]In mol (mol Ti)$^{-1}$

[e]Efficiency of H_2O_2 = (amount of product / amount of H_2O_2 consumed) * 100%

[f]Data were from conventional method [24]

to enter the framework during the crystallization process, resulting in a long crystallization period, low titanium content in the framework and a large amount of non-framework titanium. In contrast, in this work, piperidine and isopropanol were used as protective agents innovatively to avoid the transitional hydrolysis of titanium species during evaporation before crystallization certainly.

Combined with the analysis above, the proposed mechanism for the formation of nanosized Ti-MWW is depicted in Fig. 12. During the conventional dry gel procedure, the synthetic gel precursor turned to produce white solids when TOBT was added into aqueous solution, which can be ascribed to precipitation of TiO_2 (the Ti species are no longer available for incorporation into the framework once the TiO_2 is formed) [30]. However, in this basic media, the synthetic gel contained TBOT turned to be sol phase in the synergistic effect between PI and IPA avoiding the precipitation of TiO_2. Hence, based on this phenomenon, we give a detail explanation of the incorporation of Ti into framework of Ti-MWW zeolite and the formation of mesoporous and microporous structure during crystallization.

Here, the Ti-MWW with superior activity is generated in a multistep process: (a) The cluster of TOBT is dispersed into IPA to avoid the instantaneous hydrolysis by direct contact with aqueous solution; (b) under alkaline conditions, TBOT is captured and protected by PI, a slow hydrolysis process of TBOT occurs with the progressing of aging and evaporation, and a small part of SiO_2 is dissolved into monomeric silicate species and small silica oligomers (four to six silicon atoms) synchronously [35]. Then the hydrolysate combine with monomeric silicate species, leading to the formation of Si–O-Ti–O-Si bonds instead of Ti–O-Ti bonds [29]; (c) the precursor tends to be dry gel after aging and evaporation, Ti species protected by PI were dispersed evenly in it to participate in the subsequent crystallization, and the seeds dispersed in dry–gel plays a role in inducing crystallization in the subsequent process; (d) the dry gel transferred into an autoclave; during the period of crystallization, the synchronous reaction is as follows (i)-(ii): (i) In the continuous circulation of water-PI steam, a continuous liquid film of water-PI would form on the surface of solid phase, which would lead to the dissolution and crystallization of SiO_2, the PI protecting TBOT located in the aggregation pores of silica evaporate to form a thin liquid-film cover around the Ti sites simultaneously, this would produce local concentration raise and lead to the dissolution and rearrangement of the silica around the Ti species. Then the dissolved small silica particles rearrange and convert into connected flaky structure with the dual efforts of nucleation induced by seeds and continuous circulation of water-PI steam, and in the meanwhile, the Ti species would merge into MWW framework in situ; (ii) then these nanocrystals migrate and accumulate under the action of liquid-film to form irregular intermediate voids with the crystallization period prolong and eventually establish the mesopores; (e) intrinsic micropores are exposed by removing the PI remained in framework, and the 3D structure is established.

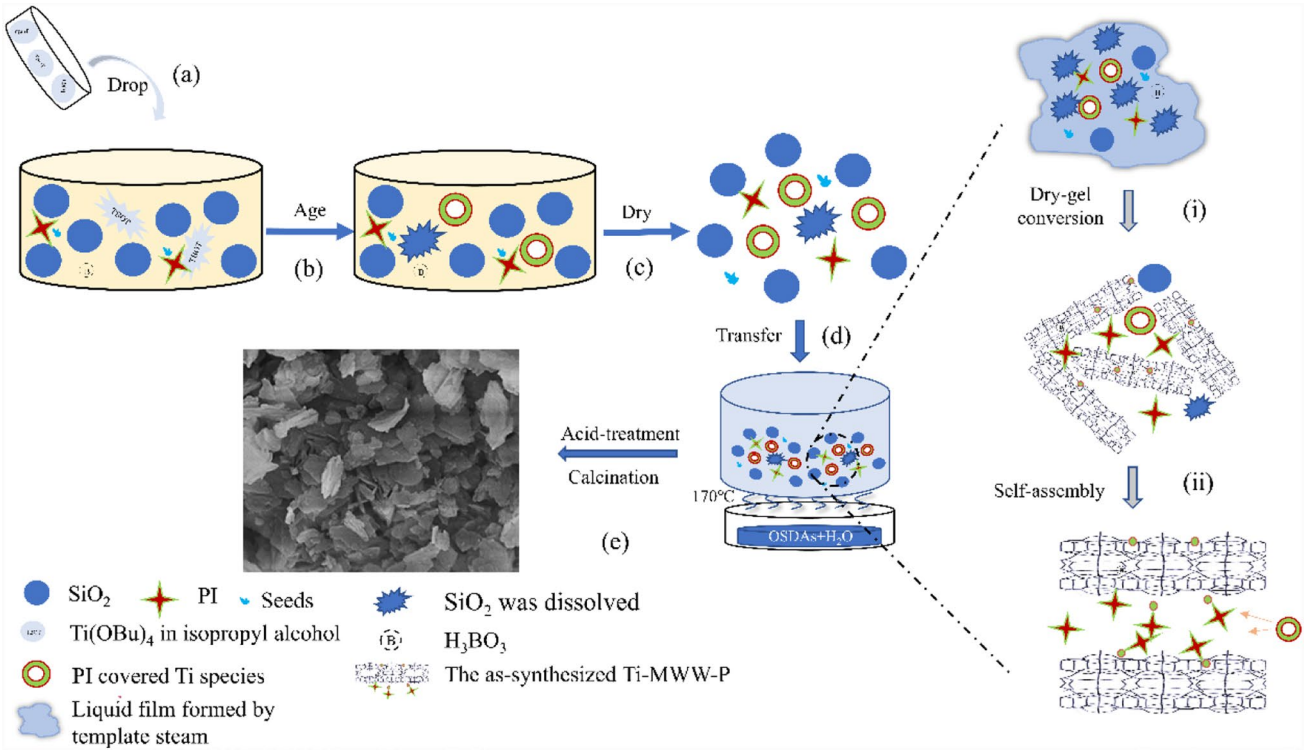

Fig. 12 Scheme: A schematic diagram for possible formation mechanism of Ti-MWW zeolite synthesized by this facile method

4 Conclusion

In this study, Ti-MWW with crystal size in the 200–400 nm range and the intracrystalline mesopores around 20 nm have been directly synthesized via a one-step steam-environment crystallization strategy without post-treatment. In comparison with conventional dry gel method, this method not only shorten the crystallization period from 7 to 2 d which greatly reduced the energy consumption, but also improve the incorporation of Ti species in framework structure. Importantly, the catalytic tests show that the nanosized Ti-MWW exhibit a higher activity almost 7 times of that of conventional Ti-MWW-DGC zeolite's in the epoxidation of 1-hexene.

Based on characterizations, the formation mechanism of one-step fast synthesis of Ti-MWW with steam-environment crystallization method was investigated. The formation of Ti-MWW with high activity was attributed to the synergistic effect between piperidine and isopropanol which improve the utilization of effective titanium species and avoid its hydrolysis into titanium dioxide. With the dual efforts of nucleation induced by seeds and continuous circulation of water-PI steam, the silica particles covered with liquid-film dissolve, rearrange, grown, migrate and accumulate to form Ti-MWW zeolites with irregular intermediate voids, which would improve the accessibility of active sites. Meanwhile, the Ti species protected by PI would merge into MWW framework in situ, greatly reducing the crystallization period of Ti-MWW. Moreover, the facile and effective strategy demonstrates in this paper would be promising to be used in developing other layered zeolites with high catalytic performance.

Acknowledgements Sincerely acknowledges the support of National Natural Science Foundation of China (No. 21571036) and Department of education, Fujian province (No: JT180397).

Compliance with Ethical Standards

Conflict of interest There is no conflict of interests in submission of this manuscript, and the manuscript is also approved by all authors for publication. I would like to declare on behalf of my co-authors that the work described was original research that has not been published previously, and not under consideration for publication elsewhere, in whole or in part. All the authors listed have approved the manuscript that is enclosed.

References

1. Moliner M, Martinez C, Corma A (2015) Multipore zeolites: synthesis and catalytic applications. Angew Chem Int Ed 54:3560–3579
2. Jiang J, Jorda JL, Yu J, Baumes LA, Mugnaioli E, Diaz-Cabanas MJ, Kolb U, Corma A (2011) Synthesis and structure determination of the hierarchical meso-microporous zeolite ITQ-43. Science 333:1131–1134

3. Moliner M (2014) State of the art of Lewis acid-containing zeolites: lessons from fine chemistry to new biomass transformation processes. Dalton Trans 43:4197–4208
4. Notari B (1996) Microporous crystalline titanium silicates. Adv Catal 41:253–334
5. Wu P, Tatsumi T, Komatsu T, Yashima T (2000) Hydrothermal synthesis of a novel titanosilicate with MWW topology. Chem Lett 29:774–775
6. Fan W, Wu P, Namba S, Tatsumi T (2004) A titanosilicate that is structurally analogous to an MWW-type lamellar precursor. Angew Chem Int Ed 43:236–240
7. Wu P, Tatsumi T, Komatsu T, Yashima T (2001a) A novel titanosilicate with MWW structure. I. Hydrothermal synthesis, elimination of extraframework titanium, and characterizations. J Phys Chem B 105(15):2897–2905
8. Wu P, Tatsumi T, Komatsu T, Yashima T (2001b) A novel titanosilicate with MWW structure: II. Catalytic properties in the selective oxidation of alkenes. J Catal 202:245–255
9. Wu P (2003) A novel titanosilicate with MWW structure III. Highly efficient and selective production of glycidol through epoxidation of allyl alcohol with H2O2. J Catal 214:317–326
10. Moliner M, Corma A (2014) Advances in the synthesis of titanosilicates: from the medium pore TS-1 zeolite to highly-accessible ordered materials. Microporous Mesoporous Mat 189:31–40
11. Barth JO, Kornatowski J, Lercher JA (2002) Synthesis of new MCM-36 derivatives pillared with alumina or magnesia-alumina. J Mater Chem 12:369–373
12. Barth J-O, Jentys A, Iliopoulou EF, Vasalos IA, Lercher JA (2004) Novel derivatives of MCM-36 as catalysts for the reduction of nitrogen oxides from FCC regenerator flue gas streams. J Catal 227:117–129
13. Schwanke AJ, Balzer R, Wittee Lopes C, Motta Meira D, Díaz U, Corma A, Pergher S (2020) Cover feature: a lamellar MWW zeolite with silicon and niobium oxide pillars: a catalyst for the oxidation of volatile organic compounds. Chem A Eur J 26(46):10363–10363
14. Kim SJ, Jung KD, Joo OS (2004) Synthesis and Characterization of Gallosilicate molecular sieve with the MCM-22 framework topology. J Porous Mater 11(4):211–218
15. Fan W, Wu P, Namba S, Tatsumi T (2006) Synthesis and catalytic properties of a new titanosilicate molecular sieve with the structure analogous to MWW-type lamellar precursor. J Catal 243:183–191
16. Jin F, Chen S-Y, Jang L-Y, Lee J-F, Cheng S (2014) New Ti-incorporated MCM-36 as an efficient epoxidation catalyst prepared by pillaring MCM-22 layers with titanosilicate. J Catal 319:247–257
17. Jin F, Chang C-C, Yang C-W, Lee J-F, Jang L-Y, Cheng S (2015) New mesoporous titanosilicate MCM-36 material synthesized by pillaring layered ERB-1 precursor. J Mater Chem A 3:8715–8724
18. Wang L, Liu Y, Xie W, Wu H, Li X, He M, Wu P (2008) Improving the hydrophobicity and oxidation activity of Ti-MWW by reversible structural rearrangement. J of Phys Chem C 112:6132–6138
19. Xu L, Huang DD, Li CG (2015) Construction of unique six-coordinated titanium species with an organic amine ligand in titanosilicate and their unprecedented high efficiency for alkene epoxidation. Chem Commun (Camb) 51:9010–9013
20. Guo S, Ye YZY, Song J, Li M (2020) MWW-type Titanosilicate synthesized by simply treating ERB-P zeolite with acidic H_2TiF_6 and Its catalytic performance in a liquid Epoxidation of 1-Hexene with H_2O_2. Acs Omega 5:9912–9919
21. Wu P, Tatsumi T (2002) Preparation of B-free Ti-MWW through reversible structural conversion. Chem Commun. https://doi.org/10.1039/b201170k
22. Davis ME (2013) Zeolites from a materials chemistry perspective. Chem Mater 26:239–245
23. Wu Q, Liu X, Zhu L, Ding L, Gao P, Wang X, Pan S, Bian C, Meng X, Xu J, Deng F, Maurer S, Muller U, Xiao FS (2015) Solvent-free synthesis of zeolites from anhydrous starting raw solids. J Am Chem Soc 137:1052–1055
24. Wu P, Miyaji T, Liu Y, He M, Tatsumi T (2005) Synthesis of Ti-MWW by a dry–gel conversion method. Catal Today 99:233–240
25. Ke X, Xu L, Zeng C, Zhang L, Xu N (2007) Synthesis of mesoporous TS-1 by hydrothermal and steam-assisteddry gel conversion techniques with the aid of triethanolamine. Microporous Mesoporous Mat 106:68–75
26. Chen X, Meng X, Xiao F-S (2015) Solvent-free synthesis of SAPO-5 zeolite with plate-like morphology in the presence of surfactants. Chin J Catal 36:797–800
27. Wang X, Wu Q, Chen C, Pan S, Zhang W, Meng X, Maurer S, Feyen M, Muller U, Xiao FS (2015) Atom-economical synthesis of a high silica CHA zeolite using a solvent-free route. Chem Commun (Camb) 51:16920–16923
28. Zhang SL, Jin SQ, Tao GJ, Wang ZD, Liu W, Chen Y, Luo J, Zhang B, Sun HM, Wang YD, Yang WM (2017) The evolution of titanium species in boron-containing Ti-MWW zeolite during post-treatment revealed by UV resonance Rarnan spectroscopy. Microporous Mesoporouss Mat 253:183–190
29. Thangaraj A, Eapen MJ, Sivasanker S, Ratnasamy P (1992) Studies on the synthesis of titanium, TS-1. Zeolites 12:943–950
30. Thangaraj A, Sivasanker S (1992) An improved method for TS-1 synthesis- 29Si NMR studies. J Chem Soc-Chem Commun. https://doi.org/10.1039/c39920000123
31. Zhang J, Cao P, Yan H, Wu Z, Dou T (2016) Synthesis of hierarchical zeolite Beta with low organic template content via the steam-assisted conversion method. Chem Eng J 291:82–93
32. Shkuropatov AV, Knyazeva EE, Ponomareva OA, Ivanova II (2018) Synthesis of hierarchical MWW zeolites and their catalytic properties in petrochemical processes (Review). Pet Chem 58:815–826
33. Cundy CS, Forrest JO (2004) Some observations on the preparation and properties of colloidal silicalites. Microporous Mesoporous Mat 72:67–80
34. Wang B, Xu H, Zhu Z, Guan Y, Wu P (2019) Ultrafast synthesis of nanosized Ti-Beta as an efficient oxidation catalyst via a structural reconstruction method. Catal Sci Technol 9:1857–1866
35. Li MZ, Wang YC, Wu Y, Wang MQ, Zhou DH (2017) Structure and catalytic activity of a newly proposed titanium species in a Ti-YNU-1 zeolite: a density functional theory study. Catal Sci Technol 7:4105–4114
36. Zhou D, Zhang H, Zhang J, Sun X, Li H, He N, Zhang W (2014) Density functional theory investigations into the structure and spectroscopic properties of the Ti^{4+} species in Ti-MWW zeolite. Microporous Mesoporous Mat 195:216–226
37. Tang B, Dai W, Sun X, Guan N, Li L, Hunger M (2014) A procedure for the preparation of Ti-Beta zeolites for catalytic epoxidation with hydrogen peroxide. Gr Chem 16:2281–2291
38. Liu N, Liu Y, Xie W (2007) Hydrothermal synthesis of boron-free Ti-MWW with dual structure-directing agents. Stud Surf Sci Catal 170:464–469
39. Fan F, Feng Z, Li C (2010) UV Raman spectroscopic studies on active sites and synthesis mechanisms of transition metal-containing microporous and mesoporous materials. Acc Chem Res 43:378–387